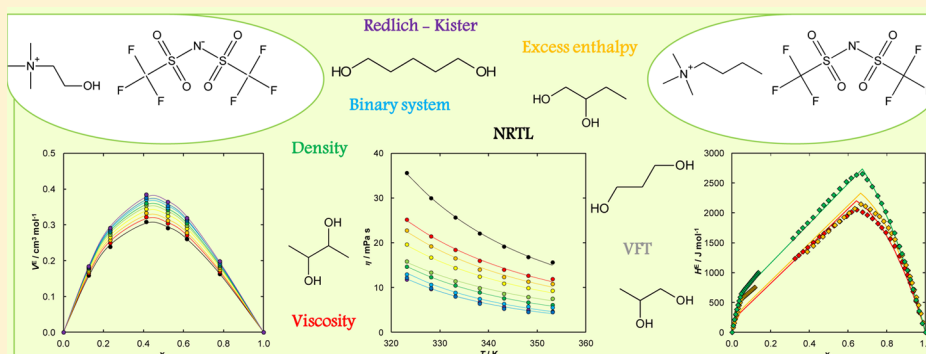


## Excess Enthalpies of Mixing, Effect of Temperature and Composition on the Density, and Viscosity and Thermodynamic Properties of Binary Systems of {Ammonium-Based Ionic Liquid + Alkanediol}

Urszula Domańska,<sup>\*,†,‡</sup> Paulina Papis,<sup>†,§</sup> Jerzy Szydłowski,<sup>§</sup> Marta Królikowska,<sup>†</sup> and Marek Królikowski<sup>†</sup><sup>†</sup>Department of Physical Chemistry, Faculty of Chemistry, Warsaw University of Technology, Noakowskiego 3, 00-664 Warsaw, Poland<sup>‡</sup>Thermodynamic Research Unit, School of Chemical Engineering, University of KwaZulu-Natal, Howard College Campus, King George V Avenue, Durban 4001, South Africa<sup>§</sup>Faculty of Chemistry, University of Warsaw, Żwirki i Wigury 101, 02-089 Warsaw, Poland

## S Supporting Information



**ABSTRACT:** In the present work the excess enthalpies of butyltrimethylammonium bis(trifluoromethyl-sulfonyl)imide,  $[N_{1114}][NTf_2]$ , with 1,2-propanediol, or 1,2-butanediol, or 2,3-butanediol have been measured at  $T = 298.15$  K. Additionally, the density,  $\rho$ , and dynamic viscosity,  $\eta$ , for binary solutions containing ionic liquids (ILs) and alkanediols, {butyltrimethylammonium bis(trifluoromethyl-sulfonyl)imide,  $[N_{1114}][NTf_2]$ , + 1,2-propanediol, 1,2-butanediol, 2,3-butanediol} and {(2-hydroxyethyl)trimethylammonium bis(trifluoro-methylsulfonyl)imide,  $[N_{1112OH}][NTf_2]$ , + 1,2-propanediol, 1,3-propanediol, 1,5-pentanediol}, at wide temperature and composition ranges at ambient pressure have been investigated. From experimental values of the density,  $\rho$ , and dynamic viscosity,  $\eta$ , the excess molar volumes,  $V^E$ , and dynamic viscosity deviations,  $\Delta\eta$ , were calculated and correlated using the Redlich–Kister polynomial equation. The temperature dependence of density and viscosity for the tested binary systems was described by an empirical second-order polynomial and by the Vogel–Fucher–Tammann equation, respectively. The variation of density and viscosity as a function of composition has been described by the polynomial correlations. Comparison of the experimental results for the binary mixtures tested in this work allows us to determine the influence of alkanediol carbon chain length, the position of the hydroxyl group in the alcohol, and the influence of the structure of the cation of the ionic liquid on the presented properties.

## ■ INTRODUCTION

For over two decades, ammonium-based ionic liquids (ILs) known as hydrophobic, air- and moisture-stable, inexpensive, and multifunctional organic salts have been an area of interest as sustainable and “green” solvents both in industrial processes<sup>1–4</sup> and in catalytic reactions.<sup>5,6</sup> Ammonium-based ILs were found to have practical value as antibacterial, antifungal agents and huge potential application for wood preservation<sup>7</sup> and antielectrostatic agents.<sup>3</sup> Ammonium-based ILs are the most popular cationic surfactants, biocides, germicides, adhesion promoters in asphalt, corrosion inhibitors, and many others.<sup>4</sup> Therefore, the potential application may be expected in cosmetics, topical antiseptics, sanitizers, pharma-

ceuticals, mildew preventatives, and organophilic clays, or emulsion stabilizing agents.<sup>4</sup> Their possible use in the extraction processes has also been proposed.<sup>7–10</sup> The use of deep eutectic solvents (DESs) with ammonium-based ILs was inspired by many innovative works, where the breakdown results were obtained as entrainers or catalysts.<sup>10–17</sup> DESs including ammonium ILs {choline chloride (ChCl), tetramethylammonium chloride (TMAC), and tetrabutyl ammonium chloride (TBAC)} were chosen as typical hydrogen bond acceptors and

Received: July 1, 2014

Revised: October 9, 2014

Table 1. Structures, Names, and Abbreviations of the Ionic Liquids Studied

Structure	Name, abbreviation
	butyltrimethylammonium bis(trifluoromethylsulfonyl)imide, [N <sub>1114</sub> ][NTf <sub>2</sub> ]
	(2-hydroxyethyl)trimethylammonium bis(trifluoromethylsulfonyl)imide, [N <sub>1112OH</sub> ][NTf <sub>2</sub> ]
	1,2-propanediol
	1,3-propanediol
	1,2-butanediol
	2,3-butanediol
	1,5-pentanediol

in mixtures with malonic acid, glycerol, tetraethylene glycerol, ethylene glycol, and polyethylene glycol were used for the desulfurization of fuels successfully.<sup>10</sup> The tetrabutyl ammonium chloride/polyethylene glycol (TBAC/PEG) DES have shown the highest extraction efficiency.<sup>10</sup> DESs composed of quaternary ammonium salts were used for separation of phenols from model oils.<sup>11</sup> DESs were used with success as media in the catalyzed reactions and as catalysts for biodiesel production.<sup>13–16</sup> Ammonium ILs with special herbicidal anions are proposed as a promising herbicide efficacy.<sup>18</sup>

Ammonium-based ILs play an important role in the living process beginning at vitamins (vitamin B complex and thiamine) to enzymes, which participate in the carbohydrate and choline metabolism. The most popular, choline chloride, [N<sub>1112</sub>OH][Cl], salt. It is crucial for several biological functions.<sup>19</sup> Synthesis of several choline chloride derivatives<sup>20–22</sup> and the interaction with alcohols, water, ethers, and many others were presented in the open literature.<sup>21–29</sup>

Choline-based ILs are known as less toxic and more biodegradable alternatives to popular imidazolium- or pyridinium-based ILs.<sup>30,31</sup> Special attention has been paid in recent years to study the fundamental physicochemical and thermophysical properties of ammonium-based ILs and popular solvents, polyhydric alcohols and diols.<sup>31–41</sup> Only a few studies on phase equilibria of binary mixtures including choline-based ILs have been presented in the open literature.<sup>7,8,21,23–25</sup>

The liquid–liquid phase equilibrium (LLE) with upper critical solution temperature (UCST) was detected for imidazolium-based ILs with three anions [BF<sub>4</sub>]<sup>−</sup>, [PF<sub>6</sub>]<sup>−</sup>, and

[NTf<sub>2</sub>]<sup>−</sup> with diols, 1,2-ethanediol, 1,2-propanediol, 1,3-propanediol, 1,2-butanediol, 1,2-pentanediol, 1,2-hexanediol, 1,3-butanediol, 1,4-butanediol, 2,3-butanediol, 1,5-pentanediol, and 1,2,3-propanetriol.<sup>34,41</sup> This type of phase equilibria is characteristic for the miscibility behavior of ILs with the same anions, such as for example {1-ethyl-1-methylpiperidinium bis(trifluoromethyl)sulfonyl}imide, [EMPIP][NTf<sub>2</sub>], with monohydroxyalcohols.<sup>42</sup> Usually, the increase of UCST was observed with an increase of an alcohol chain length.<sup>42</sup> In the case of 1,2-diols, miscibility with imidazolium-based ILs increases with a decrease of alkyl portion of the alcohol, passes via a maximum, and then decreases.<sup>41</sup> The relative position of the OH groups within an alcohol molecule affects the mutual solubility: the vicinal position favors the miscibility.<sup>34</sup>

Experimental determination of excess molar enthalpy of mixing,  $H^E$ , data is usually cheaper and less time-consuming than vapor–liquid equilibrium (VLE) or liquid–liquid equilibrium (LLE) measurements. In many cases, the data of VLE are at higher temperatures, where the components are chemically less stable, and  $H^E$  data (measured usually at low temperatures) are used to model the plant operation conditions. Recently, we have published the new sets of experimental data on  $H^E$  in binary systems of piperidinium-based ILs with ethanol and propan-1-ol.<sup>43</sup> The results of  $H^E$  give an insight into mutual interaction between the IL and an alcohol moieties. The  $H^E$  data for pyrrolidinium-based IL with pentane, hexane, 1-hexene, and 1-heptene were presented earlier to obtain new interaction parameters for Modified UNIFAC.<sup>44</sup> The  $H^E$  data were presented as well for binary mixtures of (imidazolium-based ILs + water).<sup>45–47</sup>

The main goal of this work is to present new sets of experimental data on excess enthalpies of mixing,  $H^E$ , in binary systems {butyltrimethylammonium bis(trifluoromethyl-sulfonyl)imide,  $[N_{1114}][NTf_2]$ , (1) + alkanediol (2)} at  $T = 298.15$  K, measured by isothermal titration calorimetry. To the best of our knowledge, this is the very first work presenting  $H^E$  of ammonium-based IL with alkanediols. This study comprises three binary systems to determine the influence of alkanediol carbon chain length and the position of the hydroxyl group in the alcohol. Additionally, the density,  $\rho$ , and the dynamic viscosity,  $\eta$ , were determined for two ammonium-based ILs with different alkanediols at wide temperature and composition range at ambient pressure. The compounds were selected in such a way that it was possible to determine the alkanediol carbon chain length, the position of the hydroxyl group in the alcohol, and the influence of the structure of the cation of the IL on the presented properties. Those data are important from the standpoint of design and optimization of chemical engineering processes involving the used chemicals. The density of the pure (2-hydroxyethyl)trimethylammonium bis(trifluoromethyl-sulfonyl)imide,  $[N_{1112OH}][NTf_2]$ , was measured earlier.<sup>29</sup>

## EXPERIMENTAL PROCEDURES

**Materials.** The studied ionic liquids, butyltrimethylammonium bis(trifluoromethyl-sulfonyl)imide,  $[N_{1114}][NTf_2]$  (CAS No. 258273-75-5), and (2-hydroxyethyl)trimethylammonium bis(trifluoromethyl-sulfonyl)imide,  $[N_{1112OH}][NTf_2]$  (CAS No. 827027-25-8), were supplied by Iolitec GmbH (Germany) and were reported to have a mass fraction purity >0.99. The purity in mass fraction and supplier of each of the solvents were as follows: 1,2-propanediol (CAS No. 57-55-6, Sigma-Aldrich,  $\geq 0.995$ ); 1,3-propanediol (CAS No. 504-63-2, Sigma-Aldrich,  $\geq 0.980$ ); 1,2-butanediol (CAS No. 584-03-2, Fluka,  $\geq 0.980$ ); 2,3-butanediol (CAS No. 513-85-9, Sigma-Aldrich,  $\geq 0.980$ ); 1,5-pentanediol (CAS No. 111-29-5, Sigma-Aldrich,  $\geq 0.970$ ).

The samples of ILs were purified by degassing using an ultrasonic bath and by subjecting the liquid to a low pressure of about 1 mPa at temperature  $T = 343$  K for 48 h to eliminate volatile compounds. No decomposition of the ILs was observed at the experimental conditions. The alkanediols were stored over freshly activated molecular sieves of type 4 Å (Union Carbide). The water mass fraction of the dried ILs was determined using Karl Fischer titration (model SCHOTT Instruments TitroLine KF), and it was found to be less than 300 ppm in mass fraction for all samples. The structures, names, and abbreviations of the ionic liquids and alkanediols tested in this work are presented in Table 1.

**Excess Enthalpy Measurements.** The isothermal titration calorimeter (ITC, model TAM III, TA Instruments, USA) was used to determine the excess molar enthalpies of mixing for  $\{[N_{1114}][NTf_2]$  (1) + 1,2-ethanediol, or 1,2-propanediol, or 1,2-butanediol, or 2,3-butanediol (2)} binary mixtures at temperature  $T = 298.15$  K. The titration and reference cells were placed in the test wells of the highly stable thermostatic oil bath. During the experiment, the temperature of the oil bath was maintained at  $T = 298.15$  K for 24 h with a stability of  $\pm 100$   $\mu$ K. The sample of 0.5 mL of pure IL was placed in the titration cell (stainless steel ampule), which was placed into the thermostatic oil bath and equilibrated for a few hours. A small amount of alkanediol was injected into the titration cell using the precise syringe pump. The mixture was rigorously stirred (100 rpm) during the titration. The number of moles of the

injected fluid was calculated from the volume with the known density and molecular weight. The measured property is the difference in heat flow between the sample and the reference cells. Summation of the integration of the individual heat flow peaks results in the total amount of heat effect during the  $j$ -th injection ( $\delta q_j$ ). This quantity is readily transformed into total molar excess enthalpy of mixing corresponding to  $i$  injections ( $H_i^E$ )

$$H_i^E = \frac{\sum_{j=1}^i \delta q_j}{n_1 + \sum_{j=1}^i \Delta n_{2,j}} \quad (1)$$

where  $n_1$  is the number of moles of the IL and  $\Delta n_{2,j}$  is the number of moles of solvent injected during the  $j$ -th titration (please note that in further text we will denote the IL and solvent as 1 and 2, respectively). The uncertainty of the  $H^E$  data determined in the present study is estimated to be less than 0.5%. In order to verify the reliability of measurements, the experiments for {methanol + water} and {cyclohexane + hexane} binary mixtures have been done. Those systems exhibit, respectively, negative and positive heat effects of mixing. The summary of the comparison of experimental results obtained by the TAM III calorimeter with literature values has been presented by us previously.<sup>43</sup>

**Density Measurements.** The density of pure compounds and tested binary mixtures was carried out using an Anton Paar GmbH 4500 vibrating-tube densimeter (Graz, Austria), thermostated at different temperatures. The densimeter includes an automatic correction for the viscosity of the sample. The densimeter's calibration was performed at atmospheric pressure using doubly distilled and degassed water and dried air. The calibration for temperature and pressure was made by the producer. The temperature uncertainty, estimated to be 0.01 K, was provided by two integrated Pt 100 platinum thermometers. The apparatus is precise to within  $1 \times 10^{-5}$  g·cm<sup>-3</sup>, and the uncertainty of the measurements was estimated to be better than  $\pm 1 \times 10^{-4}$  g·cm<sup>-3</sup>. Binary mixtures were prepared with uncertainty of  $\pm 1 \times 10^{-4}$  g by mass using a high precision analytical balance (Mettler Toledo AB204-S). In order to minimize the variation in composition, due to evaporation or absorption of water by IL, each sample was prepared immediately before the experiment. The comparison of the experimental and literature values of the density for pure ILs and alkanediols is presented in Table 2.<sup>48–56</sup>

The density of  $[N_{1114}][NTf_2]$  published up until today in the open literature is changing from 1.3236 g·cm<sup>-3</sup><sup>53</sup> to 1.3716 g·cm<sup>-3</sup><sup>48,52</sup> at  $T = 323.15$  K. Our value is 1.37066 g·cm<sup>-3</sup> and is close to the work of Deng et al.<sup>49</sup> The density of  $[N_{1112OH}][NTf_2]$  is 1.50516 g·cm<sup>-3</sup>, which is very close to the only published data 1.5044 g·cm<sup>-3</sup><sup>55</sup> at  $T = 323.15$  K. The densities of alkanediols, which are easier liquids for the purification, are very similar to the literature data.<sup>56</sup> Some higher discrepancies are for the longer chain alkanediols, 2,3-butanediol and 1,5-pentanediol, which are more viscous. As is generally known, that density depends strongly on the method of synthesis (producer), method of purification, and method of measurements.

**Dynamic Viscosity Measurements.** Viscosity measurements for pure compounds and tested binary systems were carried out using an Anton Paar GmbH AMVn (Graz, Austria) programmable viscometer, with a nominal uncertainty of  $\pm 0.1\%$  and reproducibility <0.1% for viscosities from (0.3 to

**Table 2.** Physical Properties of Pure Components at  $T = 323.15$  K: Measured Density ( $\rho$ ), Density from the Literature ( $\rho^{\text{lit}}$ ), Measured Dynamic Viscosity ( $\eta$ ), and Dynamic Viscosity from the Literature ( $\eta^{\text{lit}}$ )

compound	$\rho$ (g·cm <sup>-3</sup> )	$\rho^{\text{lit}}$ (g·cm <sup>-3</sup> )	$\eta$ (mPa·s)	$\eta^{\text{lit}}$ (mPa·s)
[N <sub>1114</sub> ][NTf <sub>2</sub> ]	1.37066	1.3716 <sup>a</sup>	35.62	34.38 <sup>a</sup>
		1.3702 <sup>b</sup>		35.5 <sup>b</sup>
		1.3696 <sup>c</sup>		37.5 <sup>c</sup>
		1.3537 <sup>d</sup>		
		1.3716 <sup>e</sup>		
		1.3236 <sup>f</sup>		
		1.3698 <sup>g</sup>		
[N <sub>1112OH</sub> ][NTf <sub>2</sub> ]	1.50516	1.5044 <sup>h</sup>	39.28	42.63 <sup>h</sup>
1,2-propanediol	1.01372	1.01352 <sup>i</sup>	12.20	12.27 <sup>i</sup>
1,3-propanediol	1.03439	1.03482 <sup>i</sup>	14.16	10.77 <sup>i</sup>
1,2-butanediol	0.97909	0.97960 <sup>i</sup>	12.85	12.74 <sup>i</sup>
2,3-butanediol	0.97609	0.96969 <sup>i</sup>	16.98	25.42 <sup>i</sup>
1,5-pentanediol	0.97149	0.97464 <sup>i</sup>	29.80	31.48 <sup>i</sup>

<sup>a</sup>Ref 48. <sup>b</sup>Ref 49. <sup>c</sup>Ref 50. <sup>d</sup>Ref 51. <sup>e</sup>Ref 52. <sup>f</sup>Ref 53. <sup>g</sup>Ref 54. <sup>h</sup>Ref 55. <sup>i</sup>Ref 56.

2500) mPa·s. Temperature was controlled internally with a precision of  $\pm 0.01$  K in a range from (293.15 to 353.15) K. In the measured viscosity range the diameter of the capillary was 1.6, 1.8, and 3.0 mm for the following viscosity ranges: (0.3 to 10) mPa·s, (2.5 to 70) mPa·s, and (20 to 230) mPa·s, respectively. The experimental dynamic viscosities of pure compounds in comparison with literature values are presented in Table 2.<sup>48–56</sup> The viscosity of the [N<sub>1114</sub>][NTf<sub>2</sub>] is very close to the one value published earlier as was the value for density.<sup>49</sup> Higher discrepancies are observed for [N<sub>1112OH</sub>][NTf<sub>2</sub>], where the measured value was 39.28 mPa·s and the literature value was 42.63 mPa·s at  $T = 323.15$  K.<sup>55</sup> The same situation occurs with 1,3-propanediol (14.6 mPa·s/10.77 mPa·s<sup>56</sup>) and 2,3-butanediol (16.98 mPa·s/25.42 mPa·s<sup>56</sup>) at  $T = 323.15$  K. The usual interpretation is purification method and water content, but the instrument used means the method of measurements is also important.

## RESULTS AND DISCUSSION

The data on  $H^E$  of binary systems {[N<sub>1114</sub>][NTf<sub>2</sub>] + 1,2-propanediol, or 1,2-butanediol, or 2,3-butanediol} at temperature  $T = 298.15$  K were presented to give fundamental information about the interaction in the solution. Additionally, the excess molar volumes and viscosity deviations were calculated from the density,  $\rho$ , and the dynamic viscosity,  $\eta$ , measurements for binary solutions containing ILs {[N<sub>1114</sub>][NTf<sub>2</sub>] + 1,2-propanediol, 1,2-butanediol, 2,3-butanediol} and {[N<sub>1112OH</sub>][NTf<sub>2</sub>] + 1,2-propanediol, 1,3-propanediol, 1,5-pentanediol} at wide temperature and composition ranges at ambient pressure. These data give the additional information about the interaction between used chemicals.

**Excess Enthalpy Data.** The excess molar enthalpies, of three {[N<sub>1114</sub>][NTf<sub>2</sub>] (1) + 1,2-propanediol, or 1,2-butanediol, or 2,3-butanediol (2)} binary mixtures have been determined at  $T = 298.15$  K and  $P = 0.1$  MPa. The experimental data are shown in Figure 1. The presentation for individual alkanediols is shown in Figures 1S–3S, and the numerical data are shown in Table 1S in the Supporting Information (SI).

The excess molar enthalpy values for all the studied binary mixtures are positive (endothermic effect) and do not reflect a strong interaction between the IL and alkanediol. The overall

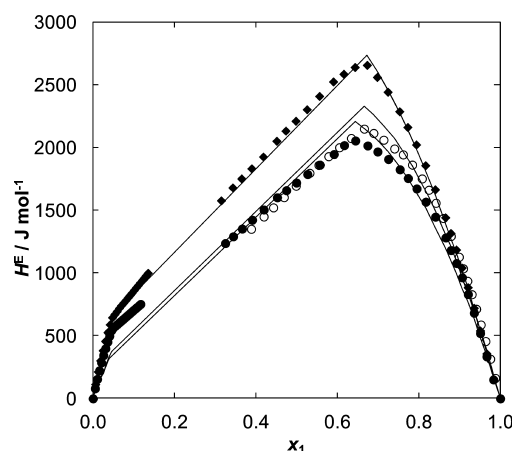


**Figure 1.** Plot of the experimental and calculated excess enthalpy,  $H^E$ , as a function of ionic liquid mole fraction,  $x_1$ , at temperature  $T = 298.15$  K in the binary mixtures {[N<sub>1114</sub>][NTf<sub>2</sub>] (1) + alkanediol (2)}: (●) 1,2-propanediol; (○) 1,2-butanediol; (◆) 2,3-butanediol; solid lines represent NRTL equation with parameters given in Table 3.

**Table 3.** Correlation Parameters of the  $H^E$  Data in the Systems of {[N<sub>1114</sub>][NTf<sub>2</sub>] (1) + 1,2-Propanediol, or 1,2-Butanediol, or 2,3-Butanediol (2)} Using the NRTL<sup>a</sup> Equation and Standard Deviation,  $\sigma^b$

compound	$g_{12} - g_{22}/(\text{J}\cdot\text{mol}^{-1})$	$g_{21} - g_{11}/(\text{J}\cdot\text{mol}^{-1})$	$\sigma/(\text{J}\cdot\text{mol}^{-1})$
1,2-propanediol	8796.7	2084.2	98
1,2-butanediol	10130.2	1873.2	103
2,3-butanediol	5169.4	10379.9	35

<sup>a</sup>  $\alpha = 0.5$ . <sup>b</sup> Given by the equation  $\sigma = [\sum_{i=1}^n \{(H_{\text{exp}}^E - H_{\text{calc}}^E)^2 / (n - k)\}]^{1/2}$ .

magnitude of  $H^E$  for these mixtures results from a positive effect due to the breakdown of the alkanediol–alkanediol interaction or IL–IL interaction. It means that the interactions between like molecules are more preferable than interactions between the IL–alkanediol. It is generally known from the previous papers of alkanediols with ILs that there is an immiscibility gap in such mixtures.<sup>34,41</sup> The shape of presented  $H^E$  curves confirms this type of interaction in binary systems at temperature  $T = 298.15$  K. The odd behavior observed between  $x_1 = 0$  and  $x_1 = 0.1$ , and in the mole fraction region near the maximum, is a result of the immiscibility gap in these binary systems in the liquid phase. The  $H^E$  curves are not symmetric in the whole mole fraction region, and the maximum is shifted to the larger mole fraction of the IL. The maximum of the  $H^E$  is 2054 J·mol<sup>-1</sup> ( $x_1 = 0.64$ ), 2149 J·mol<sup>-1</sup> ( $x_1 = 0.67$ ), and 2656 J·mol<sup>-1</sup> ( $x_1 = 0.67$ ) for 1,2-propanediol, 1,2-butanediol, and 2,3-butanediol, respectively. Even though the differences in  $H^E$  are relatively small, we can deduce some trends governing an impact of structure of alkanediols. In particular, from experimental results it can be observed that with an increase of the alkyl chain length in alkanediols the values of the  $H^E$  slightly increases, while the change of substitution of the hydroxyl group from position 1,2 to 2,3 in the butanediol causes a significant increase in the  $H^E$  value. The maximum of  $H^E$  has changed about +100 J·mol<sup>-1</sup> when changing from 1,2-propanediol to 1,2-butanediol, whereas  $H^E$  has changed about +600 J·mol<sup>-1</sup> when changing from 1,2-propanediol to 2,3-butanediol and about +500 J·mol<sup>-1</sup> when changing from 1,2-butanediol to 2,3-butanediol. One can



**Table 4.** Experimental Density,  $\rho$ , Excess Molar Volume,  $V^E$ , Dynamic Viscosity,  $\eta$ , and Dynamic Viscosity Deviation,  $\Delta\eta$ , for the {[N<sub>1114</sub>][NTf<sub>2</sub>] (1) + 1,2-Propanediol (2)} Binary System at Atmospheric Pressure ( $P = 0.1$  MPa)<sup>a</sup>

T (K)	$x_1$								
	1.0000	0.8680	0.8091	0.6946	0.4726	0.2738	0.1851	0.1157	0.0000
	$\rho$ (g·cm <sup>-3</sup> )								
323.15	1.37066	1.35568	1.34769	1.33065	1.28603	1.22040	1.17628	1.13096	1.01372
328.15	1.36629	1.35125	1.34329	1.32625	1.28156	1.21596	1.17195	1.12675	1.00979
333.15	1.36194	1.34686	1.33889	1.32185	1.27718	1.21154	1.16765	1.12252	1.00586
338.15	1.35762	1.34245	1.33452	1.31749	1.27269	1.20711	1.16338	1.11825	1.00187
343.15	1.35331	1.33805	1.33016	1.31311	1.26822	1.20266	1.15899	1.11395	0.99782
348.15	1.34900	1.33365	1.32584	1.30869	1.26376	1.19823	1.15465	1.10965	0.99375
353.15	1.34471	1.32924	1.32150	1.30413	1.25932	1.19377	1.15036	1.10529	0.98966
	$V^E$ (cm <sup>3</sup> ·mol <sup>-1</sup> )								
323.15	0.0000	0.2744	0.4370	0.5798	0.6114	0.5174	0.3923	0.2105	0.0000
328.15	0.0000	0.2893	0.4477	0.5925	0.6371	0.5420	0.4083	0.2190	0.0000
333.15	0.0000	0.3003	0.4619	0.6083	0.6526	0.5659	0.4222	0.2298	0.0000
338.15	0.0000	0.3203	0.4750	0.6205	0.6843	0.5897	0.4308	0.2412	0.0000
343.15	0.0000	0.3399	0.4872	0.6364	0.7123	0.6133	0.4483	0.2516	0.0000
348.15	0.0000	0.3595	0.4916	0.6589	0.7382	0.6338	0.4596	0.2607	0.0000
353.15	0.0000	0.3850	0.5031	0.7089	0.7629	0.6580	0.4654	0.2747	0.0000
	$\eta$ (mPa·s)								
323.15	35.62	25.18	22.76	19.63	15.85	14.66	12.95	11.79	12.20
328.15	29.97	21.44	19.21	16.72	13.36	12.33	10.63	9.67	9.85
333.15	25.66	18.42	16.53	14.35	11.41	10.46	8.85	8.04	8.00
338.15	22.08	15.98	14.01	12.44	9.87	8.91	7.45	6.68	6.41
343.15	19.16	13.99	12.36	10.89	8.60	7.59	6.35	5.62	5.27
348.15	16.81	12.65	11.32	9.89	7.89	6.68	5.76	4.96	4.54
353.15	15.63	11.91	10.80	9.30	7.51	6.10	5.53	4.62	4.51
	$\Delta\eta$ (mPa·s)								
323.15	0.00	-7.35	-8.38	-8.83	-7.41	-6.17	-3.586	-2.65	0.00
328.15	0.00	-5.88	-6.92	-7.11	-6.00	-4.94	-2.950	-2.19	0.00
333.15	0.00	-4.91	-5.76	-5.91	-4.93	-4.06	-2.420	-1.60	0.00
338.15	0.00	-4.03	-5.08	-4.85	-3.94	-3.27	-1.854	-1.24	0.00
343.15	0.00	-3.34	-4.15	-4.03	-3.24	-2.80	-1.492	-0.96	0.00
348.15	0.00	-2.54	-3.15	-3.18	-2.74	-2.39	-1.316	-0.70	0.00
353.15	0.00	-2.26	-2.71	-2.94	-2.26	-1.86	-1.042	-0.68	0.00

<sup>a</sup>Standard uncertainties  $u$  are as follows:  $u(x_1) = \pm 1 \times 10^{-4}$ ;  $u(\rho) = \pm 1 \times 10^{-4}$  g·cm<sup>-3</sup>;  $u_r(\eta) = \pm 0.1\%$ ; and  $u(T) = \pm 0.01$  K.

suppose that lower interaction with the IL (larger values of  $H^E$ ) is predicted with more hydrophobic character of 1,2-butanediol and 2,3-butanediol in comparison with 1,2-propanediol. An impact of the position of hydroxyl groups is similar, although the differences in  $H^E$  are five times larger. This trend seems to indicate also a decreasing packing order with increasing chain length of alkanediol.

The measured excess enthalpies were correlated with the NRTL equation describing the function according to the formula<sup>57</sup>

$$\frac{H^E}{RT} = -x_1x_2[N_{12}(\alpha\tau_{12} - \alpha x_1N_{12} - 1) + 1 - N_{21}(\alpha\tau_{21} - \alpha x_2N_{21} - 1)] \quad (2)$$

where

$$\tau_{12} = (g_{12} - g_{22})/RT \quad (3)$$

$$\tau_{21} = (g_{21} - g_{11})/RT \quad (4)$$

$$G_{12} = \exp(-\alpha_{12}\tau_{12}) \quad (5)$$

$$G_{21} = \exp(-\alpha_{12}\tau_{21}) \quad (6)$$

$$N_{12} = \frac{\tau_{12}G_{12}}{x_1G_{12} + x_2} \quad (7)$$

$$N_{21} = \frac{\tau_{21}G_{21}}{x_2G_{21} + x_1} \quad (8)$$

The results are shown in Table 3, where the binary parameters and the absolute arithmetic mean deviation obtained by minimizing the sum of the deviation between the experimental and calculated  $H^E$  values using Marquardt's maximum-neighborhood method are presented.<sup>58</sup>

The standard deviation  $\sigma$ /(J·mol<sup>-1</sup>) is reported in its nonreduced form, which ignores the effect of the experimental uncertainty. This form implies the same uncertainty for all data points and in many cases overestimates the values of standard deviation.

#### Effect of Temperature on the Density and Viscosity.

The experimental data of density,  $\rho$ , and dynamic viscosity,  $\eta$ , as a function of mole fraction,  $x_1$ , at different temperatures at ambient pressure are collected in Tables 4–9 for two ILs [N<sub>1114</sub>][NTf<sub>2</sub>] and [N<sub>1120H</sub>][NTf<sub>2</sub>].

From these data it can be noticed that both densities and viscosities of pure compounds and binary mixtures decrease with an increasing temperature. Fit parameters  $a_i$  with  $R^2 = 1$

**Table 5.** Experimental Density,  $\rho$ , Excess Molar Volume,  $V^E$ , Dynamic Viscosity,  $\eta$ , and Dynamic Viscosity Deviation,  $\Delta\eta$ , for the  $\{[N_{1114}][NTf_2] \text{ (1)} + 1,2\text{-Butanediol (2)}\}$  Binary System at Atmospheric Pressure ( $P = 0.1 \text{ MPa}$ )<sup>a</sup>

$T \text{ (K)}$	$x_1$							
	1.0000	0.7709	0.6457	0.4884	0.3711	0.1378	0.0969	0.0000
	$\rho \text{ (g}\cdot\text{cm}^{-3}\text{)}$							
323.15	1.37066	1.33526	1.31026	1.26965	1.22976	1.10815	1.07680	0.97909
328.15	1.36629	1.33082	1.30581	1.26521	1.22527	1.10377	1.07236	0.97515
333.15	1.36194	1.32638	1.30140	1.26079	1.22105	1.09972	1.06873	0.97118
338.15	1.35762	1.32201	1.29700	1.25637	1.21672	1.09553	1.06456	0.96717
343.15	1.35331	1.31766	1.29259	1.25193	1.21236	1.09129	1.06036	0.96311
348.15	1.34900	1.31330	1.28822	1.24752	1.20796	1.08701	1.05611	0.95903
353.15	1.34471	1.30897	1.28385	1.24312	1.20356	1.08273	1.05186	0.95491
	$V^E \text{ (cm}^3\cdot\text{mol}^{-1}\text{)}$							
323.15	0.0000	0.2854	0.3650	0.4598	0.4962	0.1972	0.1043	0.0000
328.15	0.0000	0.3022	0.3847	0.4803	0.5263	0.2229	0.1394	0.0000
333.15	0.0000	0.3219	0.3996	0.4987	0.5196	0.2110	0.0879	0.0000
338.15	0.0000	0.3328	0.4157	0.5184	0.5279	0.2119	0.0898	0.0000
343.15	0.0000	0.3406	0.4334	0.5399	0.5381	0.2143	0.0906	0.0000
348.15	0.0000	0.3499	0.4436	0.5560	0.5527	0.2196	0.0951	0.0000
353.15	0.0000	0.3751	0.4553	0.5708	0.5665	0.2220	0.0964	0.0000
	$\eta \text{ (mPa}\cdot\text{s)}$							
323.15	35.62	22.47	19.09	16.94	15.53	13.55	13.23	12.85
328.15	29.97	19.06	16.13	14.18	13.27	10.93	10.70	10.30
333.15	25.66	16.35	13.78	12.01	11.03	8.96	8.68	8.33
338.15	22.08	14.17	11.92	10.29	9.35	7.44	7.12	6.83
343.15	19.16	12.41	10.40	8.90	8.10	6.26	5.98	5.65
348.15	16.81	10.93	9.13	7.77	7.02	5.32	5.19	4.75
353.15	15.63	10.09	8.39	7.12	6.33	4.78	4.58	4.03
	$\Delta\eta \text{ (mPa}\cdot\text{s)}$							
323.15	0.00	−7.93	−8.46	−7.02	−5.76	−2.43	−1.82	0.00
328.15	0.00	−6.41	−6.88	−5.72	−4.33	−2.0770	−1.50	0.00
333.15	0.00	−5.34	−5.74	−4.79	−3.73	−1.76	−1.34	0.00
338.15	0.00	−4.41	−4.75	−3.99	−3.13	−1.48	−1.18	0.00
343.15	0.00	−3.66	−3.97	−3.35	−2.56	−1.25	−0.98	0.00
348.15	0.00	−3.12	−3.40	−2.87	−2.20	−1.09	−0.73	0.00
353.15	0.00	−2.88	−3.13	−2.57	−2.00	−0.84	−0.58	0.00

<sup>a</sup>Standard uncertainties  $u$  are as follows:  $u(x_1) = \pm 1 \times 10^{-4}$ ;  $u(\rho) = \pm 1 \times 10^{-4} \text{ g}\cdot\text{cm}^{-3}$ ;  $u_r(\eta) = \pm 0.1\%$ ; and  $u(T) = \pm 0.01 \text{ K}$ .

for the empirical correlation (see eqs 9 and 10) of the density as a function of temperature are listed in Tables 2S and 3S in the SI, for  $[N_{1114}][NTf_2]$  and  $[N_{1112OH}][NTf_2]$ , respectively, and a function of concentration ( $b_i$ ) for pure substances and for mixtures is listed in Tables 4S and 5S in the SI, for  $[N_{1114}][NTf_2]$  and  $[N_{1112OH}][NTf_2]$ , respectively

$$\rho = a_2 T^2 + a_1 T + a_0 \quad (9)$$

$$\rho = b_4 x_1^4 + b_3 x_1^3 + b_2 x_1^2 + b_1 x_1 + b_0 \quad (10)$$

The density and viscosity of both ILs are larger than those of alkanediols. The density of  $[N_{1112OH}][NTf_2]$ , for example, ranges in values from  $1.51434 \text{ g}\cdot\text{cm}^{-3}$  at  $T = 313.15 \text{ K}$  ( $\rho = 1.51198 \text{ g}\cdot\text{cm}^{-3}$ )<sup>29</sup> to  $1.47803 \text{ g}\cdot\text{cm}^{-3}$  at  $T = 353.15 \text{ K}$  and that of 1,2-propanediol from  $1.01372 \text{ g}\cdot\text{cm}^{-3}$  at  $T = 313.15 \text{ K}$  to  $0.98966 \text{ g}\cdot\text{cm}^{-3}$  at  $T = 353.15 \text{ K}$ .

The data are presented in Figures 2 and 3 (temperature dependency) and in Figures 4 and 5 (concentration dependency) for one chosen binary mixture of  $[N_{1114}][NTf_2]$  and  $[N_{1112OH}][NTf_2]$ , respectively. The further data are shown in Figures 4S–12S in the SI.

The viscosity decreases with a decrease of the IL content. Dynamic viscosity of the pure IL and the mixtures as a function of temperature through the composition range was correlated

by the well-known Vogel–Fulcher–Tammann (VFT) equation.<sup>59,60</sup>

$$\eta = CT^{0.5} \exp\left(\frac{D}{T - T_0}\right) \quad (11)$$

The fit parameters, determined empirically are in general  $C$ ,  $D$ , and  $T_0$  when the linear relation is observed between the logarithmic value of  $\eta T^{0.5}$  and  $(T - T_0)^{-1}$  according to eq 11 with three adjustable parameters. Because the glass transition temperatures,  $T_g$ , of both ILs were not detected, the ideal transition temperature,  $T_0$  was added as an optimized parameter. The values of  $T_0$  for  $[N_{1114}][NTf_2]$  and  $[N_{1112OH}][NTf_2]$  are equal to 137.77 and 135.88 K, respectively. One value of parameter  $T_0$  was used for different concentrations. The fit parameters are presented in Tables 6S and 7S in the SI for  $[N_{1114}][NTf_2]$  and  $[N_{1112OH}][NTf_2]$ , respectively. Figures 6 and 7 depict the dynamic viscosity as a function of temperature for  $\{[N_{1114}][NTf_2] \text{ (1)} + 1,2\text{-propanediol (2)}\}$  and  $\{[N_{1112OH}][NTf_2] \text{ (1)} + 1,3\text{-propanediol (2)}\}$  as examples. The remaining binary systems are shown in Figures 13S–16S in the SI. The temperature dependence of viscosity becomes distinctly nonlinear, especially at high IL content. The parameters  $C$

**Table 6.** Experimental Density,  $\rho$ , Excess Molar Volume,  $V^E$ , Dynamic Viscosity,  $\eta$ , and Dynamic Viscosity Deviation,  $\Delta\eta$ , for the  $\{[N_{1114}][NTf_2] \text{ (1)} + 2,3\text{-Butanediol (2)}\}$  Binary System at Atmospheric Pressure ( $P = 0.1 \text{ MPa}$ )<sup>a</sup>

$T \text{ (K)}$	$x_1$							
	1.0000	0.9121	0.6863	0.5485	0.4430	0.3784	0.1858	0.0000
	$\rho \text{ (g}\cdot\text{cm}^{-3}\text{)}$							
323.15	1.37066	1.35809	1.31769	1.28484	1.25356	1.23090	1.13762	0.97609
328.15	1.36629	1.35367	1.31329	1.28037	1.24914	1.22644	1.13318	0.97185
333.15	1.36194	1.34928	1.30884	1.27590	1.24469	1.22201	1.12874	0.96754
338.15	1.35762	1.34489	1.30440	1.27146	1.24025	1.21755	1.12428	0.96322
343.15	1.35331	1.34045	1.29985	1.26702	1.23525	1.21322	1.11962	0.95883
348.15	1.34900	1.33620	1.29557	1.26261	1.23125	1.20858	1.11521	0.95443
353.15	1.34471	1.33187	1.29114	1.25819	1.22675	1.20402	1.11068	0.94999
	$V^E \text{ (cm}^3\cdot\text{mol}^{-1}\text{)}$							
323.15	0.0000	0.1586	0.4697	0.5774	0.5840	0.5441	0.3327	0.0000
328.15	0.0000	0.1678	0.4721	0.5896	0.5872	0.5523	0.3393	0.0000
333.15	0.0000	0.1743	0.4840	0.6010	0.5929	0.5538	0.3412	0.0000
338.15	0.0000	0.1867	0.4984	0.6109	0.5994	0.5612	0.3457	0.0000
343.15	0.0000	0.1903	0.5086	0.6188	0.6118	0.5666	0.3567	0.0000
348.15	0.0000	0.1959	0.5168	0.6214	0.6237	0.5755	0.3610	0.0000
353.15	0.0000	0.2010	0.5303	0.6261	0.6353	0.5920	0.3652	0.0000
	$\eta \text{ (mPa}\cdot\text{s)}$							
323.15	35.62	28.81	20.93	18.19	16.54	16.03	15.29	16.98
328.15	29.97	24.40	17.75	15.32	13.60	13.26	12.34	13.13
333.15	25.66	20.92	15.23	13.10	11.67	11.09	10.19	10.34
338.15	22.08	18.13	13.22	11.32	10.00	9.39	8.53	8.27
343.15	19.16	15.83	11.16	9.89	8.68	8.03	7.33	6.70
	$\Delta\eta \text{ (mPa}\cdot\text{s)}$							
323.15	0.00	−5.16	−8.84	−9.0	−8.69	−8.00	−5.16	0.00
328.15	0.00	−4.09	−6.94	−7.05	−6.99	−6.24	−3.92	0.00
333.15	0.00	−3.39	−5.63	−5.64	−5.45	−5.05	−3.00	0.00
338.15	0.00	−2.73	−4.53	−4.53	−4.39	−4.11	−2.31	0.00
343.15	0.00	−2.24	−4.09	−3.65	−3.54	−3.38	−1.68	0.00

<sup>a</sup>Standard uncertainties  $u$  are as follows:  $u(x_1) = \pm 1 \times 10^{-4}$ ;  $u(\rho) = \pm 1 \times 10^{-4} \text{ g}\cdot\text{cm}^{-3}$ ;  $u_r(\eta) = \pm 0.1\%$ ; and  $u(T) = \pm 0.01 \text{ K}$ .

and  $D$  from eq 11 change smoothly with composition for all systems.

The VFT equation suitably correlates, as a function of the temperature, not only the viscosities of the pure IL but also the viscosities of the mixtures for the binary systems through the composition range. Dynamic viscosity of the  $[N_{1114}][NTf_2]$  has changed from 35.62 mPa·s at  $T = 323.15 \text{ K}$  to 15.63 mPa·s at  $T = 353.15 \text{ K}$  and for 1,2-propanediol from 12.20 mPa·s at  $T = 323.15 \text{ K}$  to 4.51 mPa·s. The values of viscosity presented in this work for  $[N_{1112OH}][NTf_2]$  (39.28 mPa·s at  $T = 323.15 \text{ K}$ ) are higher than that presented for  $[N_{1114}][NTf_2]$  (35.62 mPa·s at  $T = 323.15 \text{ K}$ ) and lower than presented in the literature (42.65 mPa·s at  $T = 323.15 \text{ K}$ ).<sup>55</sup>

The composition dependence of viscosity was described by polynomial (12)

$$\eta = c_4x_1^4 + c_3x_1^3 + c_2x_1^2 + c_1x_1 + c_0 \quad (12)$$

Parameters of the correlation are listed in Tables 8S and 9S in the SI. The character of changes of experimental dynamic viscosities together with solid lines calculated with polynomial equation as a function of composition for the tested binary systems are presented in Figures 17S–19S for  $[N_{1114}][NTf_2]$  and in Figures 20S–22S for  $[N_{1112OH}][NTf_2]$  in the SI. The unusual negative synergistic effect of miscibility on the dynamic viscosity is observed in two systems:  $\{[N_{1114}][NTf_2] + 2,3\text{-butanediol}\}$  and  $\{[N_{1112OH}][NTf_2] + 1,5\text{-pentanediol}\}$ . The minimum of dynamic viscosity as a function of mole fraction in the binary mixtures was observed, especially at low temper-

atures. As we mentioned in the first part of this work, the  $H^E$  in binary system of  $\{[N_{1114}][NTf_2] + 2,3\text{-butanediol}\}$  was the highest in comparison with two other mixtures (at lower temperature). This is no doubt the result of the specific interactions in the solution between like molecules. It may be the breakdown of the van der Waals interaction between alkane chains of longer diols or the breakdown of the hydrogen bonding between two  $[N_{1112OH}][NTf_2]$  molecules or/and two molecules of 1,5-pentanediol.

The influence of the cation  $[N_{1114}]^+$  vs  $[N_{1112OH}]^+$  of the IL is visible on the values of density and viscosity for the  $\{\text{IL} + 1,2\text{-propanediol}\}$  binary systems. As shown in Figures 8 and 9 the density and viscosity of the pure IL and mixtures are much higher for  $[N_{1112OH}][NTf_2]$  in comparison with  $[N_{1114}][NTf_2]$ . The introduction of the hydroxyl group instead of the ethyl group in the molecule increases the internal hydrogen bonding and changes the physicochemical properties of the IL.

Experimental excess molar volume  $V^E$  data of all binary systems are listed in Tables 4–9. The data were correlated by the well-known polynomial of Redlich–Kister (eq 13)

$$V^E = x_1(x_1 - 1) \sum_{i=0}^{i=3} A_i(1 - 2x_1)^{i-1} \quad (13)$$

$$\sigma = \left[ \sum_{i=1}^n \{(V_{\text{exp}}^E - V_{\text{calc}}^E)^2 / (n - k)\} \right]^{1/2} \quad (14)$$

**Table 7.** Experimental Density,  $\rho$ , Excess Molar Volume,  $V^E$ , Dynamic Viscosity,  $\eta$ , and Dynamic Viscosity Deviation,  $\Delta\eta$ , for the  $\{[N_{1112OH}][NTf_2] \text{ (1)} + 1,2\text{-Propanediol (2)}\}$  Binary System at Atmospheric Pressure ( $P = 0.1 \text{ MPa}$ )<sup>a</sup>

$T \text{ (K)}$	$x_1$							
	1.0000	0.7811	0.6166	0.5214	0.4133	0.2332	0.1256	0.0000
	$\rho \text{ (g}\cdot\text{cm}^{-3}\text{)}$							
313.15	1.51434	1.47575	1.43623	1.40727	1.36651	1.26962	1.18142	1.02139
318.15	1.50974	1.47115	1.43164	1.40269	1.36197	1.26523	1.17722	1.01759
323.15	1.50516	1.46657	1.42708	1.39815	1.35744	1.26084	1.17300	1.01372
328.15	1.50059	1.46198	1.42248	1.39356	1.35289	1.25641	1.16873	1.00979
333.15	1.49604	1.45743	1.41792	1.38901	1.34836	1.25200	1.16447	1.00586
338.15	1.49150	1.45289	1.41337	1.38446	1.34386	1.24757	1.16018	1.00187
343.15	1.48699	1.44835	1.40883	1.37994	1.33931	1.24314	1.15588	0.99782
348.15	1.48248	1.44385	1.40431	1.37541	1.33480	1.23870	1.15156	0.99375
353.15	1.47803	1.43936	1.39983	1.37088	1.33029	1.23427	1.14722	0.98966
	$V^E \text{ (cm}^3\cdot\text{mol}^{-1}\text{)}$							
313.15	0.0000	0.1629	0.2603	0.2938	0.3043	0.2438	0.1555	0.0000
318.15	0.0000	0.1691	0.2715	0.3067	0.3178	0.2544	0.1620	0.0000
323.15	0.0000	0.1734	0.2791	0.3155	0.3271	0.2619	0.1668	0.0000
328.15	0.0000	0.1806	0.2904	0.3279	0.3391	0.2701	0.1713	0.0000
333.15	0.0000	0.1844	0.2987	0.3379	0.3495	0.2775	0.1754	0.0000
338.15	0.0000	0.1875	0.3048	0.3450	0.3569	0.2829	0.1785	0.0000
343.15	0.0000	0.1921	0.3123	0.3529	0.3642	0.2870	0.1801	0.0000
348.15	0.0000	0.1914	0.3158	0.3582	0.3700	0.2902	0.1811	0.0000
353.15	0.0000	0.1957	0.3232	0.3665	0.3779	0.2951	0.1835	0.0000
	$\eta \text{ (mPa}\cdot\text{s)}$							
313.15	56.44	37.34	31.11	28.58	26.72	21.97	19.71	19.09
318.15	46.77	31.09	26.23	23.59	21.93	17.90	15.95	15.17
323.15	39.28	26.18	21.70	19.75	18.25	14.79	13.08	12.20
328.15	33.37	22.32	18.62	16.76	15.40	12.40	10.84	9.85
333.15	28.65	19.22	15.87	14.37	13.15	10.52	9.12	8.00
338.15	24.59	16.54	13.73	12.63	11.34	9.01	7.72	6.40
343.15	21.65	14.68	12.15	10.88	9.88	7.78	6.61	5.27
348.15	19.11	12.98	10.65	9.60	8.68	6.77	5.69	4.50
353.15	16.95	11.55	9.42	8.48	7.67	5.91	4.91	3.78
	$\Delta\eta \text{ (mPa}\cdot\text{s)}$							
313.15	0.00	−10.92	−11.01	−9.98	−7.81	−5.82	−4.06	0.00
318.15	0.00	−8.76	−8.41	−8.05	−6.29	−4.64	−3.19	0.00
323.15	0.00	−7.18	−7.20	−6.56	−5.14	−3.72	−2.52	0.00
328.15	0.00	−5.90	−5.73	−5.36	−4.18	−2.94	−1.97	0.00
333.15	0.00	−4.91	−4.86	−4.40	−3.38	−2.30	−1.48	0.00
338.15	0.00	−4.07	−3.89	−3.25	−2.58	−1.64	−0.97	0.00
343.15	0.00	−3.38	−3.22	−2.93	−2.16	−1.31	−0.71	0.00
348.15	0.00	−2.93	−2.86	−2.52	−1.86	−1.14	−0.65	0.00
353.15	0.00	−2.51	−2.48	−2.17	−1.56	−0.95	−0.53	0.00

<sup>a</sup>Standard uncertainties  $u$  are as follows:  $u(x_1) = \pm 1 \times 10^{-4}$ ;  $u(\rho) = \pm 1 \times 10^{-4} \text{ g}\cdot\text{cm}^{-3}$ ;  $u_t(\eta) = \pm 0.1\%$ ; and  $u(T) = \pm 0.01 \text{ K}$ .

where  $x_1$  is the mole fraction of the IL and  $V^E$  is the molar excess volume. The values of the parameters ( $A_i$ ) were determined using a method of least-squares. The fit parameters are summarized in Tables 10S and 11S in the SI for  $[N_{1114}][NTf_2]$  and  $[N_{1112OH}][NTf_2]$ , respectively, along with the corresponding standard deviations,  $\sigma$ , for the correlations (eq 14): where  $n$  is the number of experimental points and  $k$  is the number of coefficients. The values of  $V^E$ , as well as the Redlich–Kister fits, are plotted in Figure 10 as a function of mole fraction,  $x_1$ , at different temperatures for one mixture of  $\{[N_{1114}][NTf_2] + 2,3\text{-butanediol}\}$  as an example. The remaining binary systems are shown in Figures 23S–26S in the SI. The values of the excess molar volumes increase with an increasing temperature for all systems.

The values of excess molar volumes,  $V^E$ , of a mixture formed from two polar compounds are the result of a number of effects

which may contribute terms differing in sign. Disruption of self-association in the IL molecules, or alkanediol molecules, makes a positive contribution, but specific interaction between two dissimilar molecules makes negative contributions to  $V^E$ . The free volume effect, which depends on differences in the characteristic pressures and temperatures of the components, makes a negative contribution. Packing effects or conformational changes of the molecules in the mixtures are more difficult to categorize. However, interstitial accommodation and the effect of the condensation give further negative contributions to  $V^E$ .

The  $V^E$  exhibits positive deviations from ideality over the entire composition range. Graphs show also slightly unsymmetrical behavior of these excess molar volumes with composition. The maximum values of  $V^E$  for  $[N_{1114}][NTf_2]$  is  $0.61 \text{ cm}^3\cdot\text{mol}^{-1}$  (for  $x_1 = 0.47$ ),  $0.50 \text{ cm}^3\cdot\text{mol}^{-1}$  (for  $x_1 = 0.37$ ),



Table 8. Experimental Density,  $\rho$ , Excess Molar Volume,  $V^E$ , Dynamic Viscosity,  $\eta$ , and Dynamic Viscosity Deviation,  $\Delta\eta$ , for the  $\{[N_{1112OH}][NTf_2] \text{ (1)} + 1,3\text{-Propanediol (2)}\}$  Binary System at Atmospheric Pressure ( $P = 0.1 \text{ MPa}$ )<sup>a</sup>

T (K)	$x_1$								
	1.0000	0.8728	0.7703	0.5894	0.4288	0.3054	0.1633	0.0526	0.0000
	$\rho \text{ (g}\cdot\text{cm}^{-3}\text{)}$								
313.15	1.51434	1.49429	1.47490	1.43197	1.37902	1.32321	1.22913	1.11654	1.04077
318.15	1.50974	1.48972	1.47034	1.42745	1.37463	1.31896	1.22519	1.11305	1.03760
323.15	1.50516	1.48515	1.46580	1.42295	1.37020	1.31470	1.22124	1.10954	1.03439
328.15	1.50059	1.48060	1.46125	1.41846	1.36580	1.31040	1.21726	1.10600	1.03116
333.15	1.49604	1.47607	1.45673	1.41398	1.36141	1.30614	1.21329	1.10245	1.02792
338.15	1.49150	1.47155	1.45222	1.40951	1.35701	1.30188	1.20931	1.09888	1.02464
343.15	1.48699	1.46706	1.44774	1.40504	1.35263	1.29759	1.20531	1.09529	1.02133
348.15	1.48248	1.46259	1.44326	1.40062	1.34825	1.29333	1.20130	1.09167	1.01799
353.15	1.47803	1.45813	1.43885	1.39618	1.34389	1.28906	1.19730	1.08805	1.01463
	$V^E \text{ (cm}^3\cdot\text{mol}^{-1}\text{)}$								
313.15	0.0000	0.1497	0.2847	0.4036	0.4357	0.3561	0.2425	0.0558	0.0000
318.15	0.0000	0.1549	0.2970	0.4261	0.4589	0.3793	0.2602	0.0627	0.0000
323.15	0.0000	0.1627	0.3085	0.4471	0.4865	0.4029	0.2770	0.0687	0.0000
328.15	0.0000	0.1688	0.3225	0.4676	0.5111	0.4302	0.2957	0.0757	0.0000
333.15	0.0000	0.1748	0.3348	0.4888	0.5360	0.4545	0.3137	0.0832	0.0000
338.15	0.0000	0.1803	0.3465	0.5087	0.5613	0.4775	0.3307	0.0895	0.0000
343.15	0.0000	0.1853	0.3572	0.5310	0.5857	0.5039	0.3487	0.0957	0.0000
348.15	0.0000	0.1869	0.3676	0.5462	0.6091	0.5261	0.3659	0.1022	0.0000
353.15	0.0000	0.1959	0.3754	0.5698	0.6342	0.5519	0.3830	0.1081	0.0000
	$\eta \text{ (mPa}\cdot\text{s)}$								
313.15	56.44	47.18	39.82	30.02	24.94	22.17	20.39	19.51	20.29
318.15	46.77	39.10	33.13	25.07	20.79	18.42	16.91	16.22	16.88
323.15	39.28	32.83	27.92	21.18	17.50	15.47	14.19	13.62	14.16
328.15	33.37	27.90	23.79	18.12	14.95	13.14	12.01	11.54	12.01
333.15	28.65	23.94	20.51	15.60	12.87	11.27	10.27	9.86	10.24
338.15	24.59	20.75	17.83	13.62	11.18	9.76	8.86	8.48	8.00
343.15	21.65	18.14	15.62	11.96	9.79	8.51	7.74	7.36	7.47
348.15	19.11	16.00	13.80	10.58	8.63	7.46	6.78	6.39	6.62
353.15	16.95	14.19	12.29	9.49	7.65	6.58	5.98	5.57	5.80
	$\Delta\eta \text{ (mPa}\cdot\text{s)}$								
313.15	0.00	-4.66	-8.31	-11.58	-10.85	-9.16	-5.81	-2.68	0.00
318.15	0.00	-3.87	-6.78	-9.43	-8.90	-7.59	-4.85	-2.23	0.00
323.15	0.00	-3.26	-5.59	-7.79	-7.43	-6.36	-4.07	-1.86	0.00
328.15	0.00	-2.76	-4.68	-6.49	-6.23	-5.39	-3.49	-1.59	0.00
333.15	0.00	-2.37	-3.91	-5.48	-5.26	-4.59	-2.97	-1.34	0.00
338.15	0.00	-1.73	-2.95	-4.16	-3.93	-3.31	-1.85	-0.39	0.00
343.15	0.00	-1.70	-2.77	-3.86	-3.76	-3.28	-2.04	-0.85	0.00
348.15	0.00	-1.52	-2.44	-3.40	-3.35	-2.97	-1.89	-0.89	0.00
353.15	0.00	-1.34	-2.10	-2.88	-2.93	-2.63	-1.64	-0.81	0.00

<sup>a</sup>Standard uncertainties  $u$  are as follows:  $u(x_1) = \pm 1 \times 10^{-4}$ ;  $u(\rho) = \pm 1 \times 10^{-4} \text{ g}\cdot\text{cm}^{-3}$ ;  $u(\eta) = \pm 0.1\%$  and  $u(T) = \pm 0.01 \text{ K}$ .

and  $0.58 \text{ cm}^3\cdot\text{mol}^{-1}$  (for  $x_1 = 0.44$ ) for 1,2-propanediol, 1,2-butanediol, and 2,3-butanediol, respectively (at  $T = 323.15 \text{ K}$ ). As we can see the order is different than that from  $H^E$  measurements, where the largest values were observed for 2,3-butanediol. However, the differences are not that large for three alkanediols, and it is necessary to underline that the densities were measured at higher temperatures (above the UCST). The maximum of  $V^E$  for  $[N_{1112OH}][NTf_2]$  binary mixtures is as follows: 0.33, 0.49, and  $0.57 \text{ cm}^3\cdot\text{mol}^{-1}$  at  $x_1 = 0.41$ , 0.43, and 0.49 for 1,2-propanediol, 1,3-propanediol, and 1,5-pentanediol, respectively (at  $T = 323.15 \text{ K}$ ). From these data it can be observed that the  $V^E$  data for  $[N_{1114}][NTf_2]$  become more positive in the following order: 1,2-butanediol < 2,3-butanediol < 1,2-propanediol, while for  $[N_{1112OH}][NTf_2]$  values of  $V^E$  increase in the following order: 1,2-propanediol < 1,3-propanediol < 1,5-pentanediol. The interaction between

unlike molecules decreases with an increase of the chain length of alkanediols, especially for  $[N_{1112OH}][NTf_2]$ . The values of  $V^E$  may show also the influence of the position of the hydroxyl group in the alkanediol molecule. The maximum of  $V^E$  for  $[N_{1114}][NTf_2]$  is slightly higher for 2,3-butanediol ( $0.58 \text{ cm}^3\cdot\text{mol}^{-1}$ ) than that for 1,2-butanediol ( $0.50 \text{ cm}^3\cdot\text{mol}^{-1}$ ), which confirms the lower interaction between unlike molecules in the solution (at  $T = 323.15 \text{ K}$ ). It is better seen for the mixtures of  $\{[N_{1112OH}][NTf_2] + 1,2\text{-propanediol, or } 1,3\text{-propanediol}\}$ . The maximum of  $V^E$  is higher for 1,3-propanediol ( $0.49 \text{ cm}^3\cdot\text{mol}^{-1}$ ) than that for 1,2-propanediol ( $0.33 \text{ cm}^3\cdot\text{mol}^{-1}$ ) (at  $T = 323.15 \text{ K}$ ). The relative position of the OH groups within an alkanediol molecule affects the intermolecular interaction: the vicinal position favors the better interaction with the IL. The same effects were observed in the binary LLE phase equilibrium measurements for the imidazolium-based ILs and alkanediols.<sup>34</sup>

**Table 9.** Experimental Density,  $\rho$ , Excess Molar Volume,  $V^E$ , Dynamic Viscosity,  $\eta$ , and Dynamic Viscosity Deviation,  $\Delta\eta$ , for the  $\{[N_{1112OH}][NTf_2] \text{ (1)} + 1,5\text{-Pentenediol (2)}\}$  Binary System at Atmospheric Pressure ( $P = 0.1 \text{ MPa}$ )<sup>a</sup>

T (K)	$x_1$								
	1.0000	0.8649	0.7851	0.5855	0.4913	0.3153	0.2142	0.0929	0.0000
	$\rho \text{ (g}\cdot\text{cm}^{-3}\text{)}$								
313.15	1.51434	1.48001	1.45695	1.38827	1.34788	1.25484	1.18713	1.08194	0.97733
318.15	1.50974	1.47549	1.45247	1.38395	1.34365	1.25091	1.18342	1.07862	0.97442
323.15	1.50516	1.47096	1.44800	1.37961	1.33941	1.24694	1.17971	1.07530	0.97149
328.15	1.50059	1.46646	1.44352	1.37529	1.33519	1.24299	1.17599	1.07197	0.96855
333.15	1.49604	1.46198	1.43908	1.37100	1.33097	1.23904	1.17224	1.06862	0.96558
338.15	1.49150	1.45748	1.43464	1.36667	1.32675	1.23506	1.16849	1.06525	0.96258
343.15	1.48699	1.45302	1.43023	1.36237	1.32254	1.23110	1.16475	1.06188	0.95956
348.15	1.48248	1.44859	1.42583	1.35808	1.31834	1.22714	1.16096	1.05847	0.95653
353.15	1.47803	1.44415	1.42143	1.35382	1.31416	1.22317	1.15718	1.05507	0.95345
	$V^E \text{ (cm}^3\cdot\text{mol}^{-1}\text{)}$								
313.15	0.0000	0.2016	0.3097	0.4188	0.4955	0.4116	0.3012	0.0763	0.0000
318.15	0.0000	0.2070	0.3204	0.4371	0.5184	0.4318	0.3198	0.0861	0.0000
323.15	0.0000	0.2166	0.3318	0.4596	0.5436	0.4568	0.3375	0.0943	0.0000
328.15	0.0000	0.2229	0.3460	0.4801	0.5665	0.4793	0.3562	0.1030	0.0000
333.15	0.0000	0.2285	0.3562	0.4971	0.5898	0.5009	0.3767	0.1113	0.0000
338.15	0.0000	0.2385	0.3670	0.5197	0.6124	0.5248	0.3953	0.1191	0.0000
343.15	0.0000	0.2462	0.3769	0.5403	0.6354	0.5466	0.4122	0.1254	0.0000
348.15	0.0000	0.2489	0.3850	0.5593	0.6567	0.5678	0.4345	0.1354	0.0000
353.15	0.0000	0.2617	0.4003	0.5779	0.6777	0.5900	0.4536	0.1402	0.0000
	$\eta \text{ (mPa}\cdot\text{s)}$								
313.15	56.44	49.45	45.15	38.38	36.98	36.76	37.81	40.78	45.63
318.15	46.77	40.84	37.28	31.36	30.19	29.69	30.32	32.88	36.87
323.15	39.28	34.16	31.15	26.14	24.94	24.30	24.66	26.78	29.80
328.15	33.37	28.87	26.31	21.97	20.95	20.21	20.24	22.03	24.52
333.15	28.65	24.72	22.52	18.72	17.71	16.96	16.86	18.32	20.26
338.15	24.59	21.33	19.46	16.11	15.17	14.44	14.12	15.40	16.84
343.15	21.65	18.59	16.98	13.98	13.08	12.37	11.92	12.99	14.44
	$\Delta\eta \text{ (mPa}\cdot\text{s)}$								
313.15	0.00	-5.52	-8.97	-13.58	-13.96	-12.27	-10.11	-5.85	0.00
318.15	0.00	-4.59	-7.36	-11.30	-11.54	-10.30	-8.67	-4.91	0.00
323.15	0.00	-3.84	-6.094	-9.21	-9.51	-8.49	-7.17	-3.90	0.00
328.15	0.00	-3.31	-5.16	-7.73	-7.92	-7.11	-6.18	-3.31	0.00
333.15	0.00	-2.80	-4.32	-6.45	-6.67	-5.94	-5.20	-2.71	0.00
338.15	0.00	-2.22	-3.47	-5.27	-5.48	-4.84	-4.38	-2.15	0.00
343.15	0.00	-2.08	-3.11	-4.68	-4.90	-4.34	-4.06	-2.12	0.00

<sup>a</sup>Standard uncertainties  $u$  are as follows:  $u(x_1) = \pm 1 \times 10^{-4}$ ;  $u(\rho) = \pm 1 \times 10^{-4} \text{ g}\cdot\text{cm}^{-3}$ ;  $u(\eta) = \pm 0.1\%$ ; and  $u(T) = \pm 0.01 \text{ K}$ .

The influence of the cation  $[N_{1114}]^+$  vs  $[N_{1112OH}]^+$  of the IL may be discussed on the example of  $\{\text{IL} + 1,2\text{-propanediol}\}$ . It can be noticed that the values of  $V^E$  for  $\{[N_{1114}][NTf_2] + 1,2\text{-propanediol}\}$  are almost two times higher than those for  $\{[N_{1112OH}][NTf_2] + 1,2\text{-propanediol}\}$  at  $T = 323.15 \text{ K}$ . This is due to the presence of additional hydroxyl group in the IL cation, resulting in a stronger interaction of the  $[N_{1112OH}]^+$  cation with 1,2-propanediol and better packing effects. The strength of interactions between the IL and alkanediols is the lowest for the  $[N_{1114}]^+$  cation, and the values of  $V^E$  are the most positive at higher temperature. It has to be the result of a more efficient breakdown of similar molecule interaction than that of packing effect at higher temperature.

The values of the excess dynamic viscosity,  $\Delta\eta$ , for all systems are listed in Tables 4–9. These values were correlated with the Redlich–Kister equation

$$\Delta\eta = x_1(x_1 - 1) \sum_{i=0}^{i=3} B_i(1 - 2x_1)^{i-1} \quad (15)$$

$$\sigma_{\Delta\eta} = \left[ \sum_{i=1}^n \{(\Delta\eta_{\text{exp}} - \Delta\eta_{\text{calc}})_i^2 / (n - k)\} \right]^{1/2} \quad (16)$$

The parameters are listed in Tables 12S and 13S in the SI for  $[N_{1114}][NTf_2]$  and  $[N_{1112OH}][NTf_2]$ , respectively, along with the corresponding standard deviations,  $\sigma_{\Delta\eta}$ , for the correlations (eq 16). Figure 11 shows the negative values of the excess dynamic viscosity for this binary system  $\{[N_{1114}][NTf_2] \text{ (1)} + 1,2\text{-butanediol (2)}\}$  with  $\Delta\eta_{\text{min}}$  shifted to the higher IL mole fraction.

This graph indicates that all of the tested binary mixtures exhibit negative deviation from ideality over the entire composition range (see the remaining systems in Figures 27S and 28S for  $[N_{1114}][NTf_2]$  and Figures 29S–31S for  $[N_{1112OH}][NTf_2]$  in the SI). The values of  $\Delta\eta$  are less negative at higher temperatures. The influence of temperature is much stronger than for the  $V^E$  values. This indicates that the specific interaction between dissimilar molecules in the solution decreases with an increasing temperature. The results of the experimental dynamic viscosity deviation,  $\Delta\eta$ , confirmed the

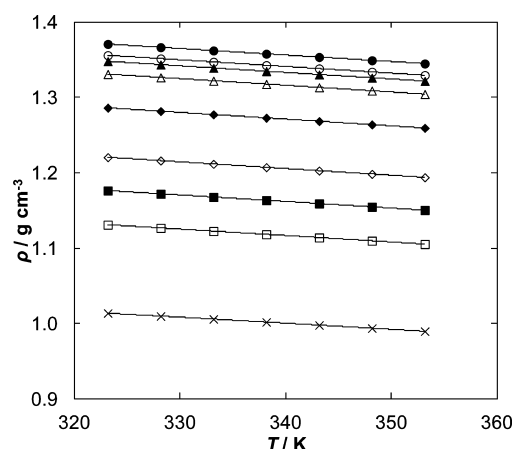


**Figure 2.** Density  $\rho$  for the  $\{[N_{1114}][NTf_2] (1) + 1,2\text{-propanediol} (2)\}$  binary mixtures as a function of temperature at concentration: (●) 1.0000; (○) 0.8680; (▲) 0.8091; (△) 0.6946; (◆) 0.4726; (◇) 0.2738; (■) 0.1851; (□) 0.1157; (×) 0.0000. Solid lines represent polynomial with parameters given in Table 2S (SI).

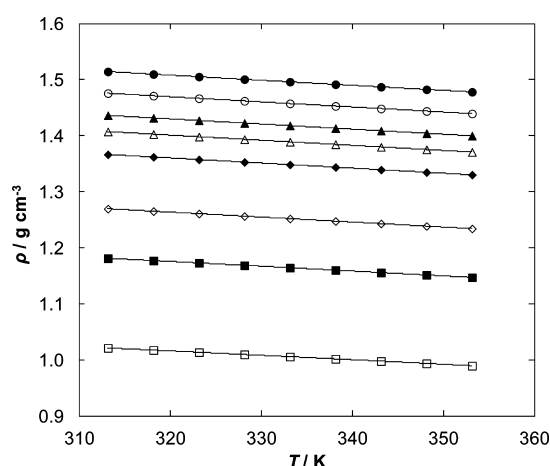


**Figure 3.** Density  $\rho$  for the  $\{[N_{1112OH}][NTf_2] (1) + 1,2\text{-propanediol} (2)\}$  binary mixtures as a function of temperature at concentration: (●) 1.0000; (○) 0.7811; (▲) 0.6166; (△) 0.5214; (◆) 0.4133; (◇) 0.2332; (■) 0.1256; (□) 0.0000. Solid lines represent polynomials with parameters given in Table 3S (SI).

conclusions obtained from the  $V^E$  values (at  $T = 323.15$  K). It was observed that the  $\Delta\eta$  data for  $[N_{1114}][NTf_2]$  became more negative in the following order: 1,2-butanediol > 1,2-propanediol > 2,3-butanediol with very small differences between alkanediols, while for  $[N_{1112OH}][NTf_2]$  values of  $\Delta\eta$  decrease in the following order: 1,2-propanediol > 1,3-propanediol > 1,5-pentanediol. The interaction between unlike molecules decreases with an increase of the chain length of alkanediols, which is better seen for  $[N_{1112OH}][NTf_2]$ . The values of  $\Delta\eta$  also show the influence of the position of hydroxyl group in the alkanediols molecules.

## CONCLUDING REMARKS

New experimental data on the excess enthalpies were detected for  $[N_{1114}][NTf_2]$  with 1,2-propanediol, 1,2-butanediol, and 2,3-butanediol binary systems at  $T = 298.15$  K. These data were correlated using the NRTL equation. The positive deviations from additivity were observed. It was confirmed that with an increase of the alkyl chain length of alkanediol the values of the  $H^E$  slightly increased, which means that the interaction between

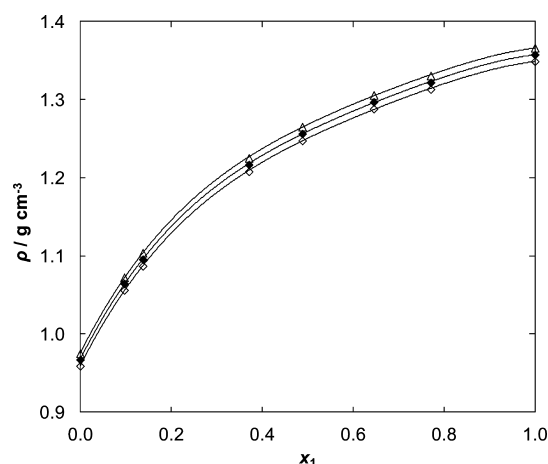


**Figure 4.** Density  $\rho$  for the  $\{[N_{1114}][NTf_2] (1) + 1,2\text{-butanediol} (2)\}$  binary mixtures as a function of concentration at different temperatures: (△) 328.15 K; (◆) 338.15 K; (◇) 348.15 K. Solid lines represent polynomial with parameters given in Table 4S (SI).

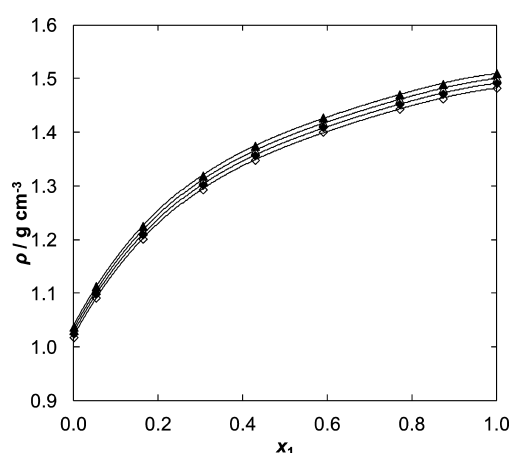


**Figure 5.** Density  $\rho$  for the  $\{[N_{1112OH}][NTf_2] (1) + 1,3\text{-propanediol} (2)\}$  binary mixtures as a function of concentration at different temperatures: (▲) 318.15 K; (△) 328.15 K; (◆) 338.15 K; (◇) 348.15 K. Solid lines represent polynomial with parameters given in Table 5S (SI).

the IL and alkanediols decreased. The change of substitution of the hydroxyl group from position 1,2 to 2,3 in the butanediol causes a significant increase in the  $H^E$  value (about  $500 \text{ J} \cdot \text{mol}^{-1}$ ).

Moreover, new data on densities and dynamic viscosities of pure ionic liquids,  $[N_{1112OH}][NTf_2]$  and  $[N_{1114}][NTf_2]$ , and alkanediols, 1,2-propanediol, 1,3-propanediol, 1,2-butanediol, 2,3-butanediol, and 1,5-pentanediol, and their binary mixtures at wide temperature and composition range were presented. From the experimental values, the excess molar volumes and dynamic viscosity deviations were calculated. The positive deviations for excess molar volumes and negative for dynamic viscosity deviations were observed. Examining the  $V^E$  data, the conclusion may be made that the interaction between unlike molecules decreases with an increase of the chain length of alkanediols, which is especially seen for  $[N_{1112OH}][NTf_2]$ . The relative position of the OH groups within an alkanediol molecule affects the intermolecular interaction: the vicinal position favors the better interaction with the IL. The influence of the cation of the IL has shown much higher interaction

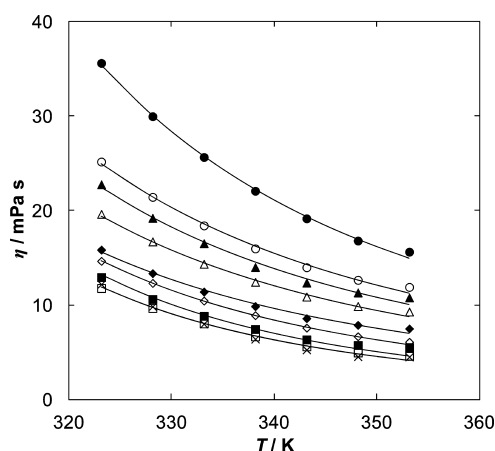


**Figure 6.** Plot of dynamic viscosity,  $\eta$ , as a function of temperature for the  $\{[N_{1114}][NTf_2] (1) + 1,2\text{-propanediol} (2)\}$  binary system at different approximated mole fractions of IL: (●) 1.0000; (○) 0.8680; (▲) 0.8091; (△) 0.6946; (◆) 0.4726; (◇) 0.2738; (■) 0.1851; (□) 0.1157; (×) 0.0000. Solid lines represent VFT equation with parameters given in Table 6S in the SI.

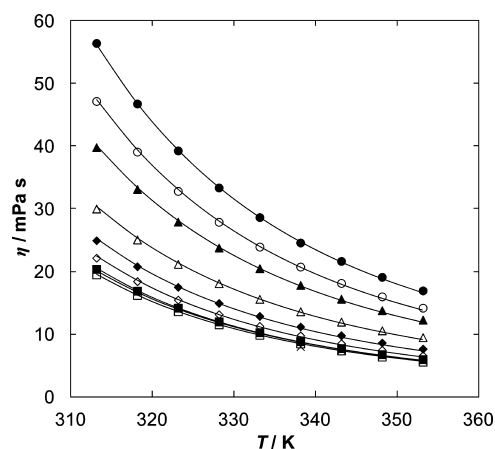


**Figure 7.** Plot of dynamic viscosity,  $\eta$ , as a function of temperature for the  $\{[N_{1112OH}][NTf_2] (1) + 1,3\text{-propanediol} (2)\}$  binary system at different approximate mole fractions of IL: (●) 1.0000; (○) 0.8728; (▲) 0.7703; (△) 0.5894; (◆) 0.4288; (◇) 0.3054; (■) 0.1633; (□) 0.0526; (×) 0.0000. Solid lines represent VFT equation with parameters given in Table 7S in the SI.

between unlike molecules for the  $[N_{1112OH}]^+$  cation. This is undoubtedly the result of a better packing effect and of the hydrogen bonding between the hydroxyl group in the cation and the alkanediol. It was noticed that the values of  $V^E$  for the  $\{[N_{1112OH}][NTf_2] + 1,2\text{-propanediol}\}$  binary system were almost two times lower than those for  $\{[N_{1114}][NTf_2] + 1,2\text{-propanediol}\}$  at  $T = 323.15$  K. Suitable correlation equations, that is second-order polynomial, Redlich–Kister, and VFT equation, were used to correlate the experimental data.

In the investigated mixtures, the more important substances were the ILs as very high hydrogen bonded substances. The positive values of the excess molar enthalpy can be explained by the disruption of the self-association of the IL and/or alkanediol. The molecular interpretation of the very weak possible cross-hydrogen bond between the IL and that of the hydroxyl group of an alkanediol at higher temperatures only are based on the picture of interactions observed by the measurements presented here, the  $H^E$ ,  $V^E$ , and  $\Delta\eta$  data. On

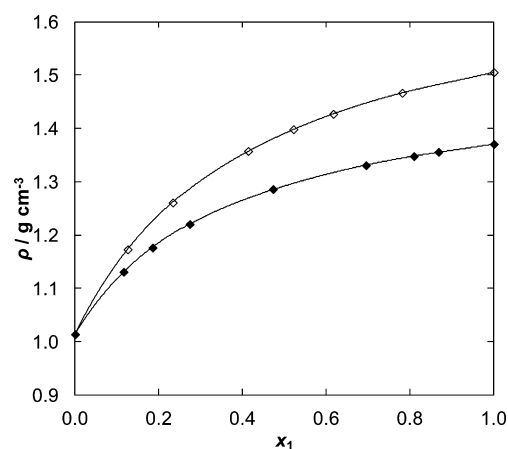


**Figure 8.** Experimental density of  $\{\text{IL} (1) + 1,2\text{-propanediol} (2)\}$  vs IL mole fraction at temperature  $T = 323.15$  K: (◆)  $[N_{1114}][NTf_2]$ ; (◇)  $[N_{1112OH}][NTf_2]$ .

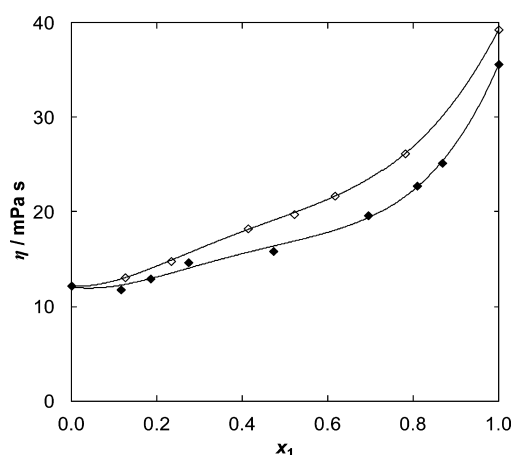


**Figure 9.** Experimental dynamic viscosity of  $\{\text{IL} (1) + 1,2\text{-propanediol} (2)\}$  vs IL mole fraction at temperature  $T = 323.15$  K: (◆)  $[N_{1114}][NTf_2]$ ; (◇)  $[N_{1112OH}][NTf_2]$ .

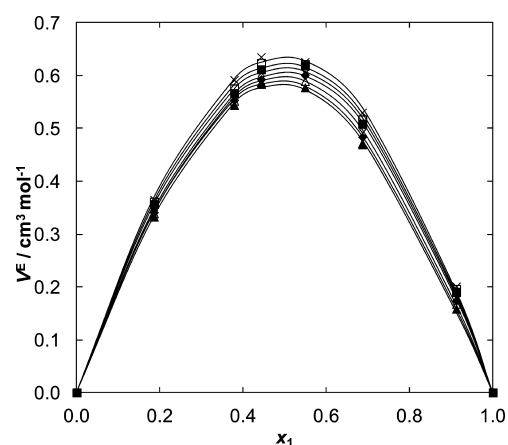


**Figure 10.** Plot of the experimental excess molar volume,  $V^E$ , as a function of ionic liquid mole fraction,  $x_1$ , at different temperatures: (▲) 323.15 K; (△) 328.15 K; (◆) 333.15 K; (◇) 338.15 K; (■) 343.15 K; (□) 348.15 K; (×) 353.15 K in the binary mixture  $\{[N_{1114}][NTf_2] (1) + 2,3\text{-butanediol} (2)\}$ . Solid lines represent the Redlich–Kister equation with parameters given in Table 10S in the SI.

the basis of the brief description of these values, the interactions in the solutions was discussed, and a detailed overview of

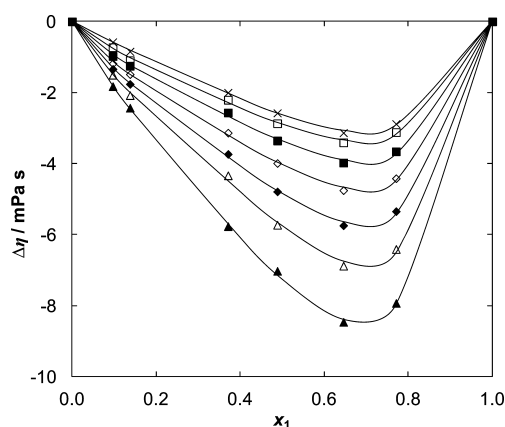


**Figure 11.** Plot of the experimental dynamic viscosity deviation,  $\Delta\eta$ , as a function of ionic liquid mole fraction,  $x_1$ , at different temperatures: (▲) 323.15 K; (△) 328.15 K; (◆) 333.15 K; (◇) 338.15 K; (■) 343.15 K; (□) 348.15 K; (×) 353.15 K in the binary mixture {[N<sub>1114</sub>][NTf<sub>2</sub>] (1) + 1,2-butanediol (2)}. Solid lines represent the Redlich–Kister equation with parameters given in Table 12S in the SI.

physicochemical properties of the investigated ILs in binary systems with alkanediols was described, which may propose the possible new applications of ammonium-based ionic liquids in the field of chemical engineering.

## ■ ASSOCIATED CONTENT

### Supporting Information

Additional figures and tables. This material is available free of charge via the Internet at <http://pubs.acs.org>.

## ■ AUTHOR INFORMATION

### Corresponding Author

\*E-mail: [ula@ch.pw.edu.pl](mailto:ula@ch.pw.edu.pl). Phone: +48226213115. Fax: +48 22 6282741.

### Notes

The authors declare no competing financial interest.

## ■ ACKNOWLEDGMENTS

This work has been supported by the Warsaw University of Technology. Author P. Papis wishes to thank for the project MPD 2010/4 “Towards Advanced Functional Materials and Novel Devices” - Joint UW and WUT International PhD Programme.

## ■ REFERENCES

- Plechova, N. V.; Seddon, K. R. Applications of Ionic Liquids in the Chemical Industry. *Chem. Soc. Rev.* **2008**, *37*, 123–150.
- Pernak, J.; Smiglak, M.; Griffin, S. T.; Hough, W. L.; Wilson, T. B.; Pernak, A.; Zabielska-Matejuk, J.; Fojutowski, A.; Kita, K.; Rogers, R. D. Long Alkyl Chain Quaternary Ammonium-Based Ionic Liquids and Potential Applications. *Green Chem.* **2006**, *8*, 798–806.
- Pernak, J. Feder-Kubis, Synthesis and Properties of Chiral Ammonium-Based Ionic Liquids. *Chem.—Eur. J.* **2005**, *11*, 4441–4449.
- Pernak, J.; Skrzypczak, A.; Lota, G.; Frackowiak, E. Synthesis and Properties of Trigeminal Tricationic Ionic Liquids. *Chem.—Eur. J.* **2007**, *13*, 3106–3112.
- Moriel, P.; García-Suárez, E. J.; Martínez, M.; García, A. B.; Montes-Morán, M. A.; Calvino-Casilda, V.; Beñares, M. A. Synthesis, Characterization and Catalytic Activity of Ionic Liquids Based on Biosources. *Tetrahedron Lett.* **2010**, *51*, 4877–4881.

- Gorke, J.; Sreinc, F.; Kazlauskas, R. Toward Advanced Ionic Liquids. Polar Enzyme-friendly Solvents for Biocatalysis. *Biotechnol. Bioprocess Eng.* **2010**, *15*, 40–53.

- Domańska, U.; Pobudkowska, A.; Żolek-Tryznowska, Z. Effect of an Ionic Liquid (IL) Cation on Ternary System (IL + p-Xylene + Hexane) at  $T = 298.15$  K. *J. Chem. Eng. Data* **2007**, *52*, 2345–2349.

- Domańska, U.; Pobudkowska, A.; Królikowski, M. Separation of Aromatic Hydrocarbons from Alkanes Using Ammonium Ionic Liquid C<sub>2</sub>NTf<sub>2</sub> at  $T = 298.15$  K. *Fluid Phase Equilib.* **2007**, *259*, 173–179.

- Wlazło, M.; Marciniak, A. Ternary Liquid-Liquid Equilibria of Trifluorotris(perfluoroethyl)phosphate Based Ionic Liquids + Benzo-thiophene + Heptane. *Fluid Phase Equilib.* **2014**, *361*, 54–59.

- Li, Ch.; Li, D.; Zou, S.; Li, Z.; Yin, J.; Wang, A.; Cui, Y.; Yao, Z.; Zhao, Z. Extraction Desulfurization Process of Fuels with Ammonium-Based Deep Eutectic Solvents. *Green Chem.* **2013**, *15*, 2793–2799.

- Guo, W.; Hou, Y.; Wu, W.; Ren, Sh.; Tian, Sh.; Marsh, K. N. Separation of Phenols of Model Oils with Quaternary Ammonium Salts via Forming Deep Eutectic Solvents. *Green Chem.* **2013**, *15*, 226–229.

- Tang, B.; Row, K. H. Recent Development in Deep Eutectic Solvents in Chemical Sciences. *Monatsh. Chem.—Chem. Mon.* **2013**, *144*, 1427–1454.

- Durand, E.; Lecomte, J.; Baréa, B.; Piombo, G.; Dubreucq, E.; Villeneuve, P. Evaluation of Deep Eutectic Solvents as New Media for Candida Antarctica Lipase B Catalyzed Reactions. *Process Biochem.* **2012**, *47*, 2081–2089.

- Hayyan, A.; Ali Hashim, M.; Mjalli, F. S.; Hayyan, M.; AlNashef, I. M. A. A Novel Phosphonium Based Deep Eutectic Catalyst for Biodiesel Production from Low Grade Crude Palm Oil. *Chem. Eng. Sci.* **2013**, *92*, 81–88.

- Lobo, H. R.; Singh, B. S.; Shankarling, G. S. Deep Eutectic Solvents and Glycerol: a Simple, Environmentally Benign and Efficient Catalyst/Reaction Media for Synthesis of N-Arylphthalimide Derivatives. *Green Chem. Lett. Rev.* **2012**, *5*, 487–533.

- Zhao, H.; Baker, G. A. Ionic Liquids and Deep Eutectic Solvents for Biodiesel Synthesis: A Review. *J. Chem. Technol. Biotechnol.* **2013**, *88*, 3–12.

- Leron, R. B.; Li, M.-H. Solubility of Carbon Dioxide in a Choline Chloride-Ethylene Glycol Based Deep Eutectic Solvent. *Thermochim. Acta* **2014**, *551*, 14–19.

- Pernak, J.; Syguda, A.; Janiszewska, D.; Materna, K.; Praczyk, T. Ionic Liquid with Herbicidal Anions. *Tetrahedron* **2011**, *67*, 4838–4844.

- Meck, W. H.; Williams, C. L. Choline Supplementation During Prenatal Development Reduces Proactive Interference in Spatial Memory. *Dev. Brain Res.* **1999**, *118*, 51–59.

- Pernak, J.; Chwała, P.; Syguda, A. Room Temperature Ionic Liquids-New Choline Derivatives. *Polym. J. Chem.* **2004**, *78*, 539–546.

- Domańska, U.; Bogel-Lukasik, R. Physicochemical Properties and Solubility of Alkyl-(2-hydroxyethyl)-dimethylammonium Bromide. *J. Phys. Chem. B* **2005**, *109*, 12124–12132.

- Domańska, U.; Bogel-Lukasik, R. Solubility of Ethyl(2-hydroxyethyl)-dimethylammonium Bromide in Alcohols (C<sub>2</sub>–C<sub>12</sub>). *Fluid Phase Equilib.* **2005**, *233*, 220–227.

- Costa, A. J. L.; Soromenho, M. R. C.; Shimizu, K.; Esperança, J. M. S. S.; Lopes, J. N. C.; Rebelo, L. P. N. Unusual LCST-type Behaviour Fund in Binary Mixtures of Choline-Based Ionic Liquids with Ethers. *RSC Adv.* **2013**, *3*, 10262–10271.

- Costa, A. J. L.; Soromenho, M. R. C.; Shimizu, K.; Marucho, I. M.; Esperança, J. M. S. S.; Lopes, J. N. C.; Rebelo, L. P. N. Liquid-Liquid Equilibrium of Cholinim-Derived Bistriflimide Ionic Liquids with Water and Octanol. *J. Phys. Chem. B* **2012**, *116*, 9186–9195.

- Nockemann, P.; Binnemans, K.; Thijs, B.; Parac-Vogt, T. N.; Merz, K.; Mudring, A. V.; Menon, P. C.; Rajesh, R. N.; Cordoyiannis, G.; Thoen, J.; et al. Temperature-Driven Miting-Demixing Behavior of Binary Mixtures of Ionic Liquid Choline Bis(trifluoromethylsilylphenyl)-imide and Water. *J. Phys. Chem. B* **2009**, *113*, 1429–1437.



- (26) Westerholt, A.; Liebert, V.; Gmehling, J. Influence of Ionic Liquids on the Separation Factor of Three Standard separation Problem. *Fluid Phase Equilib.* **2009**, *280*, 56–60.
- (27) Pereiro, A. B.; Rodriguez, A. An Ionic Liquid Proposed as Solvent in Aromatic Hydrocarbon Separation by Liquid Extraction. *AIChE J.* **2010**, *56*, 381–386.
- (28) Alonzo, L.; Arce, A.; Francisco, M.; Soto, A. Thiophene Separation from Aliphatic Hydrocarbons Using the 1-Ethyl-1-methylimidazolium Ethylsulfate Ionic Liquid. *Fluid Phase Equilib.* **2008**, *270*, 97–102.
- (29) Domańska, U.; Papis, P.; Szydłowski, J. Thermodynamics and Activity Coefficients at Infinite Dilution for Organic Solutes, Water and Diols in the Ionic Liquid Choline Bis(trifluoromethylsulfonyl)imide. *J. Chem. Thermodyn.* **2014**, *77*, 63–70.
- (30) Petkovic, M.; Ferguson, J. L.; Gunaratne, H. K. N.; Ferreira, M. C.; Leitão, S. K. R.; Rebelo, L. P. N.; Pereira, C. P. Novel Biocompatible Cholinium-Based Ionic Liquids-Toxicity and Biodegradability. *Green Chem.* **2010**, *12*, 643–649.
- (31) Weaver, K. D.; Kim, H. J.; Sun, J.; MacFarlane, D. R.; Elliott, G. D. Cyto-toxicity and Biocompatibility of a Family of Choline Phosphate Ionic Liquid designed for Pharmaceutical Applications. *Green Chem.* **2010**, *12*, 507–513.
- (32) Wagner, M.; Stanga, O.; Scroer, W. The Liquid-Liquid Coexistence of Binary Mixtures of Room Temperature Ionic Liquid 1-Methyl-3-hexylimidazolium Tetrafluoroborate with Alcohols. *Phys. Chem. Chem. Phys.* **2004**, *6*, 4421–4431.
- (33) Shiflett, M. B.; Yokozeki, A. Liquid-Liquid Equilibria in Binary Mixtures of 1,3-Propanediols + Ionic Liquids, [bmim][PF<sub>6</sub>], [bmim][BF<sub>4</sub>], and [bmim][BF<sub>4</sub>]. *J. Chem. Eng. Data* **2007**, *52*, 1302–1306.
- (34) Makowska, A.; Dyoniziak, E.; Sikorska, A.; Szydłowski, J. Miscibility of Ionic Liquids with Polyhydric Alcohols. *J. Phys. Chem. B* **2010**, *114*, 2504–2508.
- (35) Trindade, C. A. S.; Visak, Z. P.; Bogel-Lukasik, R.; Bogel-Lukasik, E.; da Ponte, M. N. Liquid–Liquid Equilibrium of Mixtures of Imidazolium-Based Ionic Liquids with Propanediol and Glycerol. *Ind. Eng. Chem. Res.* **2010**, *49*, 4850–4857.
- (36) Forte, A.; Bogel-Lukasik, E.; Bogel-Lukasik, R. Miscibility Phenomena in System Containing Polyhydroxyalcohols and Ionic Liquids. *J. Chem. Eng. Data* **2011**, *56*, 2273–2279.
- (37) Payne, S. M.; Kerton, F. M. Solubility of Bio-Sourced Feedstock in Green Solvents. *Green Chem.* **2010**, *12*, 1648–1653.
- (38) Freire, M. G.; Louros, C. L. S.; Rebelo, L. P. N.; Coutinho, J. A. P. Aqueous Biphasing Systems Composed of Water-Stable Ionic Liquid + Carbohydrates and their Applications. *Green Chem.* **2011**, *13*, 1536–1545.
- (39) Conceicao, L. J. K.; Bogel-Lukasik, E.; Bogel-Lukasik, R. A. A New Outlook on Solubility of Carbohydrates and Sugar Alcohols in Ionic Liquids. *RCS Adv.* **2012**, *2*, 1846–1855.
- (40) Carneiro, A. P.; Rodriguez, O.; Macedo, A. E. Solubility of Xylitol and Sorbitol in Ionic Liquids. Experimental Data and Modeling. *J. Chem. Thermodyn.* **2012**, *55*, 184–192.
- (41) Makowska, A.; Sztank, E.; Szydłowski, J. Liquid Phase Behavior of Hexafluorophosphate Ionic Liquids with Polyhydric Alcohols. *Fluid Phase Equilib.* **2012**, *314*, 140–145.
- (42) Domańska, U.; Królikowska, M.; Padaszyński, K. Physicochemical Properties and Phase Behaviour of Piperidinium-Based Ionic Liquids. *Fluid Phase Equilib.* **2011**, *303*, 1–9.
- (43) Padaszyński, K.; Królikowski, M.; Domańska, U. Excess Enthalpies of Mixing of Piperidinium Ionic Liquids with Short-Chain Alcohols: Measurements and PC-SAFT Modeling. *J. Phys. Chem. B* **2013**, *117*, 3884–3891.
- (44) Nebig, S.; Liebert, V.; Gmehling, J. Measurement and Prediction of Activity Coefficients at Infinite Dilution ( $\gamma^\infty$ ), Vapor-Liquid Equilibria (VLE) and Excess Enthalpies ( $H^E$ ) of Binary Systems with 1,1-Dialkyl-Pyrrolidinium Bis(trifluoromethylsulfonyl)imide using Modified UNIFAC (Dortmund). *Fluid Phase Equilib.* **2009**, *277*, 61–67.
- (45) Lindsay, E.; Ficke, H. R.; Brennecke, J. F. Heat Capacities and Excess Enthalpies of 1-Ethyl-3-methylimidazolium-Based Ionic Liquids and Water. *J. Chem. Eng. Data* **2008**, *53*, 2112–2119.
- (46) Simoni, L. D.; Lindsay, E. F.; Lambert, C. A.; Stadtherr, M. A.; Brennecke, J. F. Measurements and Prediction of Vapor-Liquid Equilibrium of Aqueous 1-Ethyl-3-methylimidazolium-Based Ionic Liquid Systems. *Ind. Eng. Chem. Res.* **2010**, *49*, 3893–3901.
- (47) García-Miñaja, G.; Troncoso, J.; Romani, L. Excess Enthalpy, Density, and Heat Capacity for Binary Systems of Alkylimidazolium-Based Ionic Liquids + Water. *J. Chem. Thermodyn.* **2009**, *41*, 161–166.
- (48) Liu, H.; Maginn, E.; Visser, A. E.; Bridges, N. J.; Fox, E. B. Thermal and Transport Properties of Six Ionic Liquids: An Experimental and Molecular Dynamics Study. *Ind. Eng. Chem. Res.* **2012**, *51*, 7242–7254.
- (49) Deng, Y.; Husson, P.; Delort, A.-M.; Besse-Hoggan, P.; Sancelme, M.; Costa Gomes, M. F. Influence of an Oxygen Functionalization on the Physicochemical Properties of Ionic Liquids: Density, Viscosity, and Carbon Dioxide Solubility as a Function of Temperature. *J. Chem. Eng. Data* **2011**, *56*, 4194–4202.
- (50) Jacquemin, J.; Husson, P.; Padua, A. A. H.; Majer, V. Density and Viscosity of Several Pure and Water-Saturated Ionic Liquids. *Green Chem.* **2006**, *8*, 172–180.
- (51) Kilaru, P.; Baker, G. A.; Scovazzo, P. Density and Surface Tension Measurements of Imidazolium, Quaternary Phosphonium, and Ammonium-Based Room-Temperature Ionic Liquids: Data and Correlations. *J. Chem. Eng. Data* **2007**, *52*, 2306–2314.
- (52) Wandschneider, A.; Lehmann, J. K.; Heintz, A. Surface Tension and Density of Pure Ionic Liquids and Some Binary Mixtures with 1-Propanol and 1-Butanol. *J. Chem. Eng. Data* **2008**, *53*, 596–599.
- (53) Wang, S.; Jacquemina, J.; Husson, P.; Hardacre, C.; Costa Gomes, M. F. Liquid–Liquid Miscibility and Volumetric Properties of Aqueous Solutions of Ionic Liquids as a Function of Temperature. *J. Chem. Thermodyn.* **2009**, *41*, 1206–1214.
- (54) Jacquemin, J.; Nancarrow, P.; Rooney, D. W.; Costa Gomes, M. F.; Husson, P.; Majer, V.; Padua, A. A. H.; Hardacre, C. Prediction of Ionic Liquid Properties. II. Volumetric Properties as a Function of Temperature and Pressure. *J. Chem. Eng. Data* **2008**, *53*, 2133–2143.
- (55) Mendonça, A. C. F.; Dörr, N.; Padua, A. A. H. Predicting Thermophysical Properties of Ionic Liquids as a Function of Temperature and Pressure. *Proc. Inst. Mech. Eng., Part J* **2013**, *226*, 965–976.
- (56) Design Institute for Physical Properties: Sponsored by AIChE DIPPR Project 801—Full Version. Design Institute for Physical Property Data/AIChE. Online version available at: <http://www.knovel.com/knovel2/Toc.jsp?BookID=1187&VerticalID=0> (2009).
- (57) Renon, H.; Prausnitz, J. M. On the Thermodynamics of Alcohol-Hydrocarbon Solutions. *Chem. Eng. Sci.* **1967**, *22*, 299–306.
- (58) Marquardt, D. An Algorithm for Least-Squares Estimation of Nonlinear Parameters. *J. Soc. Appl. Math.* **1963**, *11*, 431–439.
- (59) Fülcher, G. S. Analysis of Recent Measurements of the Viscosity of Glasses. *J. Am. Ceram. Soc.* **1925**, *8*, 339–355.
- (60) Tamman, G.; Hesse, W. Die Abhängigkeit der Viskosität von der Temperatur bei Unterkühlten Flüssigkeiten. *Z. Anorg. Allg. Chem.* **1926**, *156*, 245–257.